JAERI-Research
2002-020

HIGH EFFICIENCY, HIGH ENERGY SECOND-HARMONIC GENERATION OF Nd : GLASS LASER RADIATION IN LARGE APERTURE $CsLiB_6O_{10}$ CRYSTALS

September 2002

Hiromitsu KIRIYAMA, Norihiro INOUE and Koichi YAMAKAWA

日本原子力研究所
Japan Atomic Energy Research Institute

本レポートは、日本原子力研究所が不定期に公刊している研究報告書です。
入手の問合わせは、日本原子力研究所研究情報部研究情報課（〒319-1195　茨城県那珂郡東海村）あて、お申し越し下さい。なお、このほかに財団法人原子力弘済会資料センター（〒319-1195　茨城県那珂郡東海村日本原子力研究所内）で複写による実費頒布を行っております。

This report is issued irregularly.
Inquiries about availability of the reports should be addressed to Research Information Division, Department of Intellectual Resources, Japan Atomic Energy Research Institute, Tokai-mura, Naka-gun, Ibaraki-ken 〒319-1195, Japan.

編集兼発行　日本原子力研究所

JAERI－Research 2002－020

High Efficiency, High Energy Second-harmonic Generation of Nd:glass Laser Radiation in Large Aperture $CsLiB_6O_{10}$ Crystals

Hiromitsu KIRIYAMA, Norihiro INOUE and Koichi YAMAKAWA

Advanced Photon Research Center

Kansai Research Establishment

Japan Atomic Energy Research Institute

Kizu-cho, Souraku-gun, Kyoto

(Received July 25, 2002)

We have demonstrated the generation of a high-energy green laser pulse using large aperture $CsLiB_6O_{10}$ (CLBO) crystals. A pulsed energy of 25 J at 532-nm was generated using the 1064-nm incident Nd:glass laser radiation with an energy of 34 J. High conversion efficiency of 74 % at intensities of only 370 MW/cm^2 was obtained using a two-stage crystal architecture. This result reperesents the highest green pulse energy ever reported using the CLBO crystals. We discuss in detail the design and performance of SHG using CLBO crystals.

Keywords: Frequency Conversion, Second-harmonic Generation (SHG), Neodymium:glass Lasers, $CsLiB_6O_{10}$ (CLBO) Crystal

大口径 $CsLiB_6O_{10}$ 結晶を用いた Nd:ガラスレーザーの高効率・高エネルギー第二高調波発生

日本原子力研究所関西研究所光量子科学研究センター
桐山　博光・井上　典洋・山川　考一

(2002 年 7 月 25 日受理)

大口径 $CsLiB_6O_{10}$（CLBO）結晶を用いて高エネルギーグリーンレーザー光の発生を初めて行った。34 J の入射 1064-nm Nd:ガラスレーザー光に対して 25 J の 532-nm グリーン出力光が得られた。370 MW/cm^2 の低い入射 Nd:ガラスレーザー光強度に対して 74 %の高い変換効率を達成した。このグリーン出力エネルギーは CLBO 結晶を用いて報告されている中で最も高い値である。CLBO 結晶を用いたグリーン光の出力特性の詳細、並びに設計について議論する。

関西研究所：〒619-0215 京都府相楽郡木津町梅美台 8-1

Contents

目次

1. INTRODUCTION

Nonlinear optical crystals provide a means of extending the frequency range of available laser sources.[1,2] High power green lasers based on second- harmonic generation (SHG) of near-infrared solid-state lasers are promising for use as pump sources for Ti:sapphire chirped pulse amplification (CPA) systems. [3-5] At present the major crystals commonly used for SHG of neodymium-doped lasers are $KTiOPO_4$ (KTP), LiB_3O_5 (LBO), ß-BaB_2O_4 (BBO) and KH_2PO_4 (KDP). Though the first three crystals, KTP, LBO and BBO have large effective nonlinear coefficients,[1,2] their small crystal sizes ($\sim$1 cm^3) do not permit SHG of high energy lasers for which a large laser beam diameter is typical. The output SHG energies of the systems using these crystals are therefore limited to several hundred milijoules. The KDP crystals can be grown to a large size (> 30 cm aperture) possessing high optical quality.[6] KDP is therefore, still widely used in most high energy (tens of Joules or more) laser systems with a sacrifice of lower conversion efficiency mainly because of its small effective nonlinear coefficient. In order to obtain a modest conversion efficiency of about 50 % using the KDP crystal, the high input laser intensity level of several GW/cm^2 is required and thus close to the damage threshold of optical materials.[7]

The $CsLiB_6O_{10}$ (CLBO) crystal is a recently developed borate crystal which can be easily grown to large sizes.[8] The crystal is transparent below 200 nm and has therefore been used for generation of fourth and fifth harmonics of the neodymium-doped lasers.[9] The CLBO crystal is also phase matchable for SHG of neodymium-doped lasers and offers some attractive nonlinear properties as compared with KDP crystal.[2,10] For type II phase matching at a pump wavelength of 1064-nm, CLBO has a larger effective nonlinear coefficient (d_{eff}) and temperature bandwidth. The d_{eff} for CLBO and KDP are 0.95 pm/V and 0.38 pm/V, respectively. The temperature bandwidths for CLBO and KDP are 43.1℃ -cm and 19.1 ℃-cm, respectively. A larger d_{eff} value reduces the input laser intensity for a given SHG efficiency and also enables a shorter crystal to be used in which minimizes angular dephasing. For example, a SHG conversion efficiency of over 50 % with a green pulse energy of 1.55 J has been reported using the CLBO crystal with an input laser intensity of 360 MW/cm^2.[11] This intensity is much lower than the several GW/cm^2 levels used in previous work using the KDP crystal.[7] The large temperature bandwidth enables the crystal to be used at high average powers without significant degradation of performance. The KDP crystal has a wide angular bandwidth of 3.4 mrad-cm as compared with 1.7 mrad-cm for the CLBO crystal. The small angular bandwidth of CLBO is not, however, a limitation as its large d_{eff} value allows the use of a larger low divergence input beam at lower intensities. The walk-off angles for the CLBO and KDP crystals are rather similar. CLBO crystal dimension of $14\times11\times11$ cm^3 has been demonstrated in short

period, only three weeks and thus extra large crystal dimension is technically possible with current growth technologies. The CLBO crystal has therefore, the potential to generate high energy SHG of large aperture neodymium-doped lasers with high conversion efficiency.

In this paper we report on the generation of a high green pulse energy of 25 J with an incident energy of 34 J of Nd:glass laser using large aperture CLBO frequency doublers, corresponding to an energy conversion efficiency of 74 %. To the best of our knowledge this is the highest green output pulse energy ever produced using CLBO crystals.

2. MODEL OF SECOND-HARMONIC GENERATION

2.1 THEORY OF CONVERSION EFFICIENCY FOR SECOND-HARMONIC GENERATION

In order to gain a better understanding of the behavior of SHG conversion efficiency, we have used a numerical model based on the coupled wave equations for SHG of a monochromatic plane wave. The derivation of these equations and their solutions are given in detail in the original paper of Armstrong et al..[12] It is assumed that the beam remains locally plane over small regions, so that the plane wave solution for SHG may be used locally at each temporal and spatial point. It is also assumed that a constant value may be assigned to the dephasing across the entire beam.

The coupled wave equations for SHG are given by[12,13]

$$\frac{\partial E_2}{\partial z} = C E_1^{\,2} e^{i\Delta k z}, \tag{1}$$

$$\frac{\partial E_1}{\partial z} = -C E_2 E_1^{*} e^{-i\Delta k z}, \tag{2}$$

$$C = 5.46 d_{eff} / \lambda_1 (n_1 n_2 n_3). \tag{3}$$

where C is the nonlinear coupling constant proportional to the effective nonlinear coefficient of the crystal, Δ k is the wave vector mismatch between the input fundamental laser beam and second-harmonic output beam, d_{eff} is the effective nonlinear coefficient, λ_1 is the input fundamental laser wavelength, and n_n are refractive indices. The amplitudes are scaled as $|E_n|^2 \equiv I_n$, where I_n is the intensity. d_{eff} and λ_1 are in units of pm/V, and μm, respectively, so that the units of C is in $GW^{-1/2}$. The notation used here

is identical to that found in Ref 13.

The local conversion efficiency at a particular temporal and spatial location of the beam may be written as a function of the local drive, η_0, and the dephasing, δ [13]. The drive is the source term for the generation of the electric field at the second harmonic, and the dephasing is the phase mismatch between second-harmonic waves at the exit and entrance planes of the crystal. The conversion efficiency is given by[13]

$$\eta = \tanh^2[\frac{1}{2}\tanh^{-1}(sn[2\eta_0^{\frac{1}{2}}, 1+\delta^2/4\eta_0])], \tag{4}$$

$$\eta_0 = C^2 I L^2, \tag{5}$$

$$\delta = \frac{1}{2}\Delta k L, \tag{6}$$

where sn is an elliptic Jacobi function, I is the input fundamental laser intensity, and L is the crystal length. The Δk is primarily due to beam divergence.[13] Therefore, the Δk can be calculated as

$$\Delta k = \beta_\theta \Delta\theta, \tag{7}$$

where β_θ is the angular sensitivity and $\Delta\theta$ is the beam divergence of the input fundamental laser beam.

The familiar solution of the coupled wave equations for zero wave vector mismatch or for negligible input fundamental laser depletion are special cases of the above solution. First, for zero wave vector mismatch, Δk = 0, δ = 0, and η_0 =1. The equation (4) becomes

$$\eta = \tanh^2(\eta_0^{\frac{1}{2}}). \tag{8}$$

When the depletion of the input fundamental laser is small, we have $\eta_0 < 1$, and equation (4) becomes

$$\eta = \eta_0(\sin\delta/\delta)^2. \tag{9}$$

When the input fundamental laser fields have temporally and spatially Gaussian profiles, the following equation is more appropriate:

$$E_1(r,t) = E_0 \exp[-(t/t_0)^2 - (r/r_0)^2], \tag{10}$$

where t_0 is the pulse width and r_0 is the beam radius.

For most of the pulsed laser source, the input fundamental laser field has a temporally Gaussian profile. In this case, the input laser pulse must first be divided into a sequence of steps in time, with each step containing some known fraction of the total input fundamental laser energy. The above plane wave model can then be applied individually to each step, using the average intensity over the step size as the input fundamental intensity. In our case, the Gaussian profile was divided into several hundred steps of equal length in time. The contributions of each time step must be summed to obtain the total second harmonic energy generated in the first crystal. In the case of the second crystal in the quadrature scheme, each step in time of input laser pulse depleted in the first crystal must be applied to obtain the total second harmonic energy generated in the second crystal because the input laser beam unconverted in the first crystal is reused for further frequency conversion in the second. Then the second-harmonic fields in each crystal are assembled to obtain the total second harmonic energy generated in the two-stage architecture.

These equations allow us to estimate the harmonic conversion under ideal conditions and to anticipate certain potential problems such as a reversal of the power flow. With the equations, we have calculated the performance of the high energy SHG experiments described in Section 4.

2.2 SECOND-HARMONIC GENERATION IN CLBO

The most significant limitation to high efficiency frequency conversion of high energy pulsed laser fields is the back-conversion of the second-harmonic to the fundamental. The SHG conversion efficiency increases until a particular optimum crystal length for a given input fundamental laser intensity. Thus we optimized the both CLBO crystal lengths in the two-stage architecture for an input 1064-nm laser intensity of 400 MW/cm^2 for reliable damage-free operation. We have considered there the less specialized beams typical of tabletop laser systems as the pump laser in order to evaluate the SHG performance. The calculation assume a beam divergence of 0.5 mrad and a pulse duration of 20 ns (FWHM). The profiles of time and space are assumed to be Gaussian and flat-top, respectively. For simplicity the optical losses of the crystal and other optics are neglected. The effects of beam walk-off and bulk absorption are also neglected. We have also considered the two-stage architecture in order to achieve high conversion efficiency and to minimize back-conversion. Figure 1 shows the calculated total second-harmonic conversion efficiency as a function of input 1064-nm fundamental laser intensity in the two-stage architecture. Both first and second crystals are optimized for their lengths by using above model. The calculated optimum lengths

of the first and second crystals are 10.5 mm and 15.5 mm respectively. It is seen that the total second-harmonic conversion efficiency saturates rapidly at over 80 % for an input laser intensity of about 400 MW/cm^2. For an input intensity of only 400 MW/cm^2 the conversion efficiency predicted is as high as 82 %. The calculated suggests that high conversion efficiency is possible with low input fundamental laser intensity.

3. EXPERIMENTAL SETUP

The SHG experiments were carried out using a custom-built high power flash-lamp pumped Nd:silicate glass laser system. The schematic of the experimental setup is shown in Fig.2. This laser has a single-pass master oscillator power amplifier (MOPA) architecture. In the system a long-cavity single-longitudinal-mode 1064-nm Nd:YAG master oscillator generated pulses of about 25 ns (FWHM) duration and 200 mJ energy that were then shaped by a soft aperture to flat-top spatial profile. The shaped pulses were then amplified to 800 mJ by a Nd:YAG rod pre-amplifier of 9 mm diameter. The energy was further increased in a chain of 16, 25 and 45 mm diameter Nd: silicate glass rod amplifiers to approximately 60 J. Spatial filters were used at appropriate locations in the amplifier chain in order to reduce the intensity nonuniformity due to Fresnel diffraction. A pair of Faraday rotators were also used to prevent pulses from propagating backward down the laser chain, placed between the pre-amplifier and the 16 mm glass rod amplifier, and between the 16 mm and 25 mm glass rod amplifiers, respectively. The output temporal profile was observed to be smooth and near-Gaussian, and the spatial profile almost flat-top.

We employed a two-stage CLBO crystal architecture in order to achieve high conversion efficiency and to minimize back-conversion. A dichroic mirror placed between the two crystals separated the high power green output of the first crystal from the unconverted fundamental beam in which avoided Fresnel reflection losses of the high peak power green output in the second crystal. The dual green outputs enable the Ti:sapphire amplifier to be pumped from both sides of the Ti:sapphire crystal at lower fluence levels which avoids optical damage to the crystal faces. The individual linear polarized beams are then suitably rotated using $\lambda/2$ plates for correct orientation to the Ti:sapphire crystal in order to obtain sufficient absorption. The first and second CLBO crystals (KOGAKUGIKEN Co., Ltd) each had a cross-section of 30 mm×30 mm and their lengths were 11.5 mm and 15.5 mm, respectively. These lengths were optimized using a numerical model based on the coupled wave equations described in Section 2. The calculations assume a beam divergence of 0.4 mrad and a pulse duration of 20 ns (FWHM). The profiles of time and apace are assumed to be Gaussian and flattop, respectively. All

optical losses of the crystal and other optics are considered. Both crystals had no anti-reflection coatings. Each crystal was orientated for type II SHG of the 1064-nm input fundamental laser and was housed in a heater fitted with a proportional-integral-derivative (PID) controller. The crystals were maintained constantly at 160 ℃ with an accuracy of 0.1 ℃ and were argon gas purged in order to avoid their degradation due to stresses introduced by crystal hydration, cutting, polishing, and thermal shock owing to laser power absorption.[14] The temperature ramping rate was fixed at 2.3 ℃/min. Each heater was mounted on a precision rotating stage for optimizing the angle between the input beam and the crystal. The output beam from the glass rod amplifier chain was down-collimated to ~25 mm diameter in order to introduce it into the CLBO crystals. In all of our experiments described in this paper the temporal character of the input 1064-nm beam was monitored using a photo-diode, the incident beam energy was determined using calibrated power meter and the spatial profile was measured using charge-coupled device (CCD) camera. The output energy and spatial profile of green beam generated in each crystal were also measured using the calibrated power meter and CCD camera, respectively.

4. EXPERIMENTAL RESULTS AND DISCUSSION

Figure 3 shows the total 532-nm second-harmonic output pulse energy from the two crystals as a function of the input 1064-nm fundamental laser pulse energy. The second-harmonic output energies from each crystal are also indicated in this figure. There was no compensation for optical losses due to reflection, absorption, and scattering of the crystals. A maximum total second-harmonic output pulse energy of 25 J was obtained with 34 J of input 1064-nm fundamental laser pulse energy.

Figure 4 shows the measured and calculated 532-nm second-harmonic energy conversion efficiencies plotted as a function of the input 1064-nm laser intensity. A maximum conversion efficiency of 74 % was achieved for the dual outputs with an input laser intensity of 368 MW/cm^2. This intensity, which was calculated from the measured values of pulse duration, pulse energy and beam diameter, is much lower than the several GW/cm^2 levels used in previous work using the 10 cm aperture KDP crystal.[7] The solid, dashed and dotted curves in Fig. 4 are obtained from the coupled wave equations described in Section 2. It is seen that the experimental data are well fitted to the calculations. The agreement between the calculation curves and the data points shown in this figure indicates that our model should be able to predict the performance of a second-harmonic generator.

The results clearly demonstrate the fact that CLBO crystal is suitable for efficient

SHG of high power neodymium-doped lasers at low input intensities. The high efficiency enables effective use of energy as well as hardware. The low input intensity of less than 500 MW/cm^2 avoids intensity-dependent damage of the nonlinear crystals and other optical components.

Figure 5 shows the near-field spatial profiles of the second-harmonic beam from each crystal. The intensity distribution along the vertical and horizontal cross-sections of these beams is also shown. The near-field spatial profiles were imaged by a CCD camera through a set of image-relay optics. The beam profiles had near homogeneous flat-top spatial intensity distribution which are suitable for pumping the Ti:sapphire amplifiers without optical damage of the Ti:sapphire crystal.

5. CONCLUSION

In conclusion we have obtained 25 J of total SHG energy from 34 J of incident 1064-nm laser pulse energy using the two-stage CLBO crystal architecture. The energy conversion efficiency as high as 74 % was achieved with an input laser intensity of only 368 MW/cm^2. This scheme can be easily scaled up in energy by increasing the sizes of CLBO crystals to accommodate larger input fundamental laser beam cross-section. These experiments clearly demonstrate that the CLBO crystal, with its excellent nonlinear properties as well as availability in large sizes, is highly useful for the SHG of high-energy neodymium-doped lasers. This scheme is currently being applied for pumping an 80-mm diameter Ti:sapphire amplifier with an object to produce more than several hundred terawatt of 800-nm radiation.

ACKNOWLEDGEMENTS

The authors would like to acknowledge K. Yagi, T. Nagai, M. Aoyama and M. Fujino for their technical assistance. The authors sincerely thank Y. Kato for his encouragement and are also grateful to N. Srinivasan of Instruments Research and Development Establishment, Dehradun, India for several helpful comments on the manuscript.

REFERENCES

[1] W. Koechner, *Solid-State Laser Engineering* (Springer-Verlag, Berlin, 1996) 4th ed., p.562.

[2] V. G. Dmitriev, G. G. Gurzadyan, and D. N. Nikogosyan, Handbook of Nonlinear Optical Crystals (Springer-Verlag, Berlin, 1991) 2nd ed., p.289.

[3] A. Sullivan, J. Bonlie, D. F. Price, and W. E. White, Opt. Lett. 21, 603 (1996).

[4] J. P. Chambaret, C. Le Blanc, G. Chériaux, P. Curley, G. Darpentigny, P. Rousseau, G. Hamoniaux, A. Antonetti, and F. Salin, Opt. Lett. 21, 1921 (1996).

[5] K. Yamakawa, M. Aoyama, S. Matsuoka, T. Kase, Y. Akahane, and H. Takuma, Opt. Lett. 23, 1468 (1998).

[6] M. A. Rhodes, C. D. Boley, A. G. Tarditi, and B. S. Bauer, Proc. SPIE 2633, 94 (1995).

[7] G. J. Linford, B. C. Johnson, J. S. Hildum, W. E. Martin, K. Snyder, R. D. Boyd, W. L. Smith, C. L. Vercimak, D. Eimerl, and J. T. Hunt, Appl. Opt. 21, 3633 (1982).

[8] Y. Mori, I. Kuroda, S. Nakajima, T. Sasaki, and S. Nakai, Appl. Phys. Lett. 67, 1818 (1995).

[9] Y. K. Yap, M. Inagaki, S. Nakajima, Y. Mori, and T. Sasaki, Opt. Lett. 21, 1348 (1996).

[10] Y. Mori and T. Sasaki, Proc. SPIE 2700, 20 (1996).

[11] Y. K. Yap, S. Haramura, A. Taguchi, Y. Mori, and T. Sasaki, Opt. Commun. 145, 101 (1998).

[12] J. A. Armstrong, N. Bloembergen, J. Ducuing, and P. S. Pershan, Phys. Rev. 127, 1918 (1962).

[13] D. Eimerl, IEEE J. Quantum Electron. 23, 575 (1987).

[14] Y. K. Yap, T. Inoue, H. Sakai, Y. Kagebayashi, Y. Mori, T. Sasaki, K. Deki, and M. Horiguchi, Opt. Lett. 23, 34 (1998).

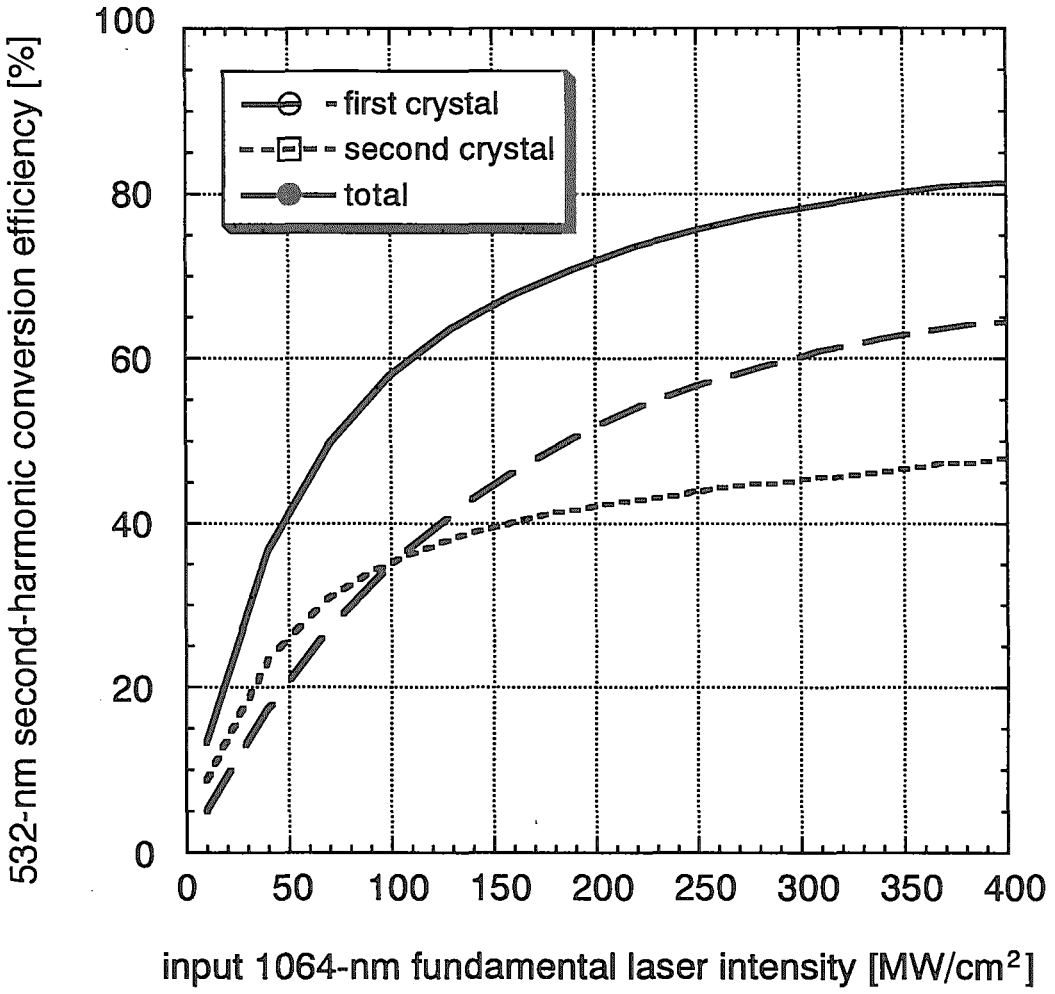

Fig.1 Calculated second-harmonic conversion efficiency as a function of 1064-nm fundamental laser intensity in two-stage architecture (solid curve). The conversion efficiencies for first crystal (dashed curve) and second crystal (dotted curve) are also shown.

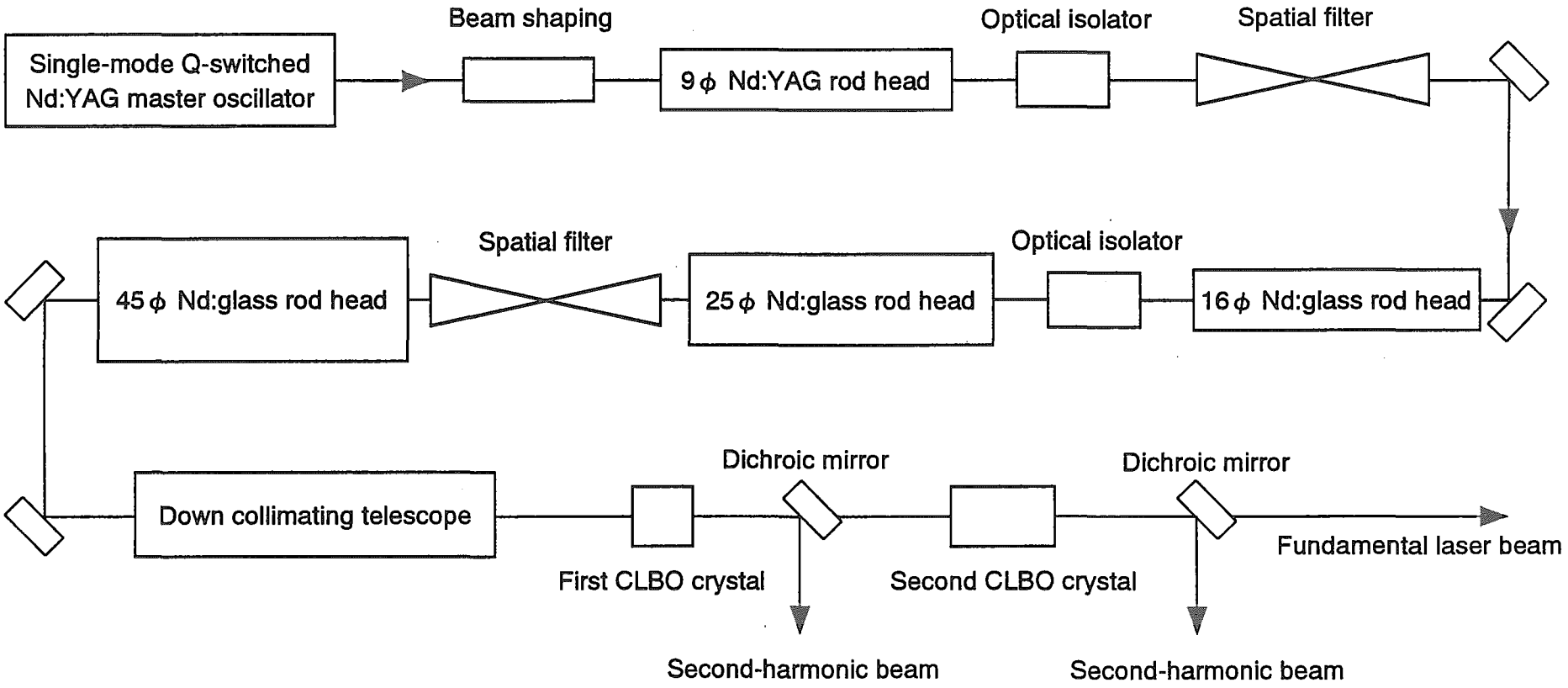

Fig.2 Schematic of the experimental setup.

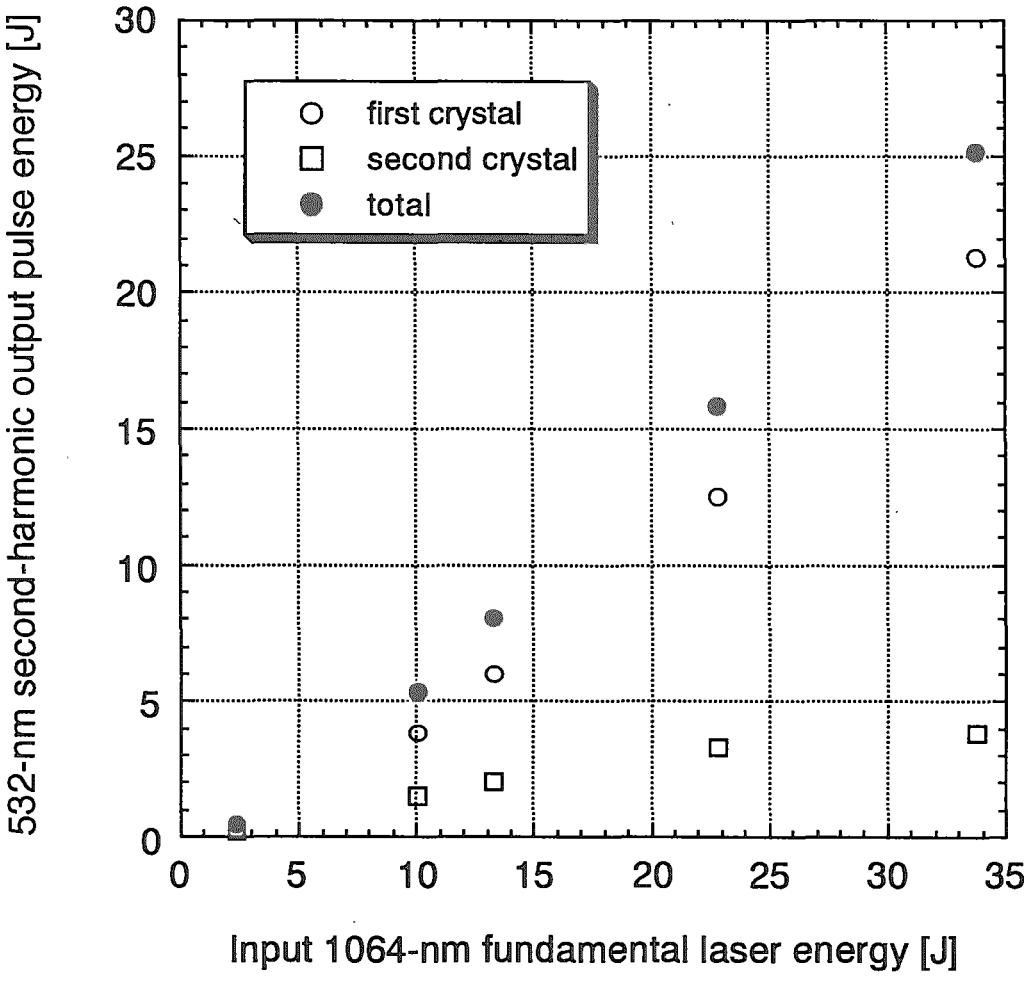

Fig.3 Total 532-nm second-harmonic output energy from both CLBO crystals versus the input 1064-nm fundamental laser energy. The energy obtained from each crystal is also shown.

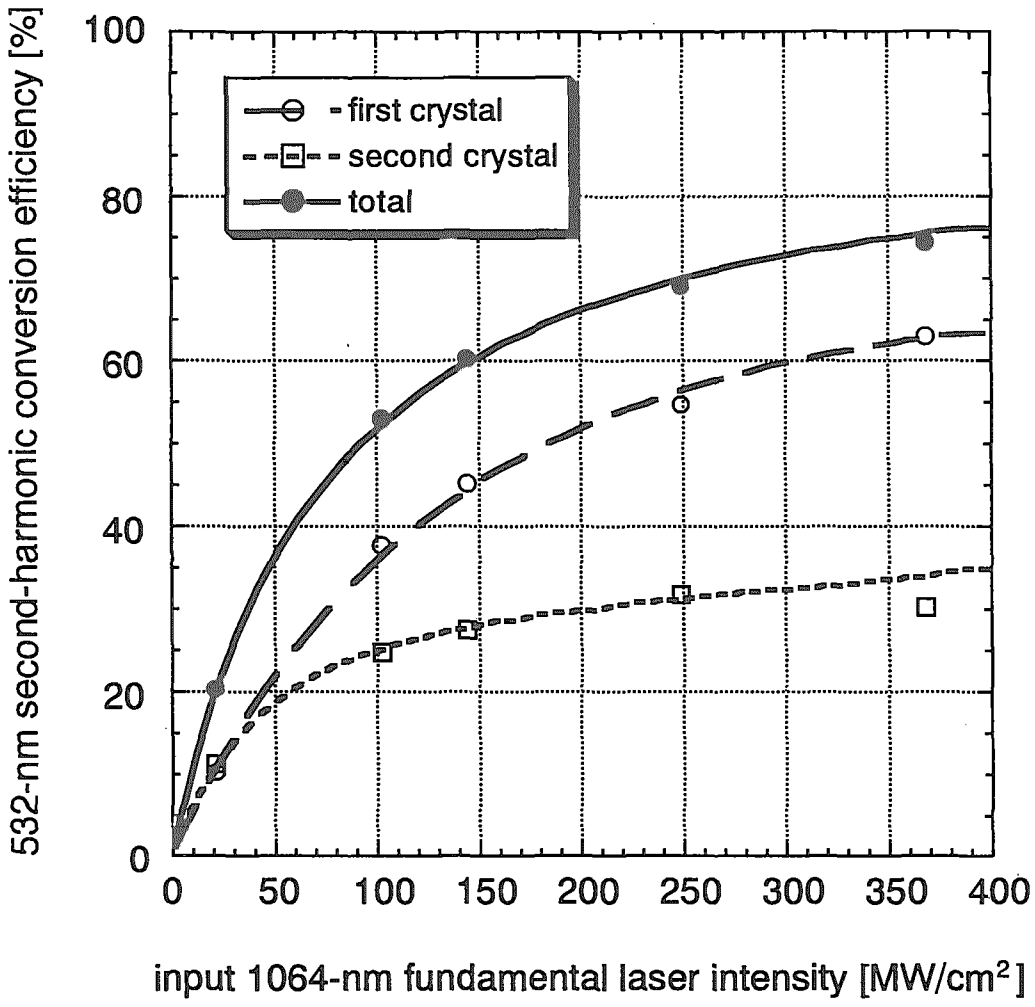

Fig.4 Measured total 532-nm second-harmonic conversion efficiency of both CLBO crystals versus the input 1064-nm fundamental laser intensity. The efficiency of each crystal is also shown. Theoretical curves for total efficiency (solid curve), for first crystal (dashed curve) and second crystal (dotted curve) as well as the corresponding data points are also shown.

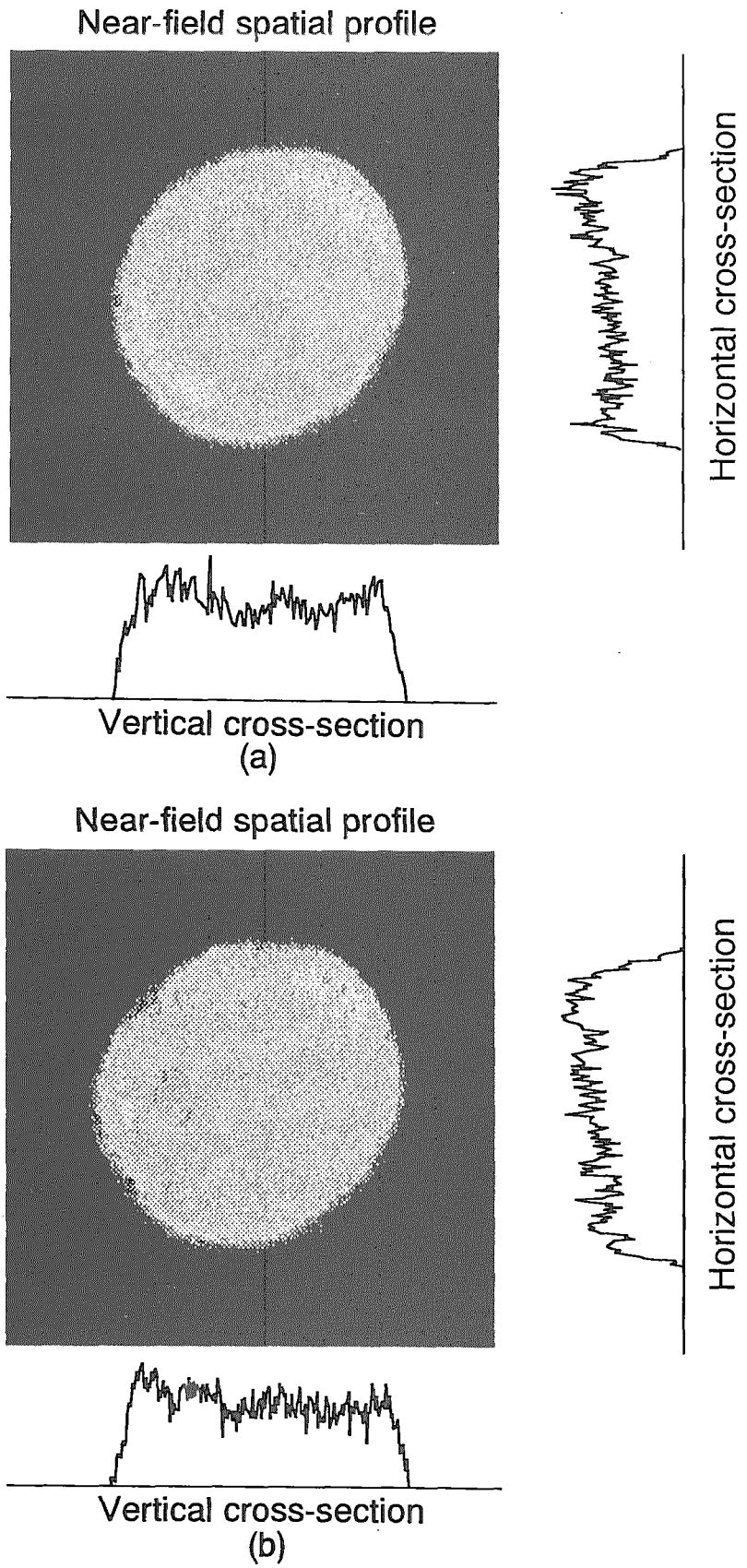

Fig.5 Near-field spatial profiles of the second-harmonic beam from each crystal. The intensity distribution along the vertical and horizontal cross sections of these beams is also shown. (a) first crystal, (b) second crystal.

This is a blank page.

国際単位系 (SI) と換算表

表1　SI基本単位および補助単位

量	名称	記号
長さ	メートル	m
質量	キログラム	kg
時間	秒	s
電流	アンペア	A
熱力学温度	ケルビン	K
物質量	モル	mol
光度	カンデラ	cd
平面角	ラジアン	rad
立体角	ステラジアン	sr

表2　SIと併用される単位

名称	記号
分，時，日	min，h，d
度，分，秒	°，′，″
リットル	l，L
トン	t
電子ボルト	eV
原子質量単位	u

1 eV=1.60218×10^{-19} J

1 u=1.66054×10^{-27} kg

表3　固有の名称をもつSI組立単位

量	名称	記号	他のSI単位による表現
周波数	ヘルツ	Hz	s^{-1}
力	ニュートン	N	m·kg/s^2
圧力，応力	パスカル	Pa	N/m^2
エネルギー，仕事，熱量	ジュール	J	N·m
工率，放射束	ワット	W	J/s
電気量，電荷	クーロン	C	A·s
電位，電圧，起電力	ボルト	V	W/A
静電容量	ファラド	F	C/V
電気抵抗	オーム	Ω	V/A
コンダクタンス	ジーメンス	S	A/V
磁束	ウェーバ	Wb	V·s
磁束密度	テスラ	T	Wb/m^2
インダクタンス	ヘンリー	H	Wb/A
セルシウス温度	セルシウス度	℃	
光束	ルーメン	lm	cd·sr
照度	ルクス	lx	lm/m^2
放射能	ベクレル	Bq	s^{-1}
吸収線量	グレイ	Gy	J/kg
線量当量	シーベルト	Sv	J/kg

表4　SIと共に暫定的に維持される単位

名称	記号
オングストローム	Å
バーン	b
バール	bar
ガル	Gal
キュリー	Ci
レントゲン	R
ラド	rad
レム	rem

1 Å= 0.1 nm=10^{-10} m

1 b=100 fm^2=10^{-28} m^2

1 bar=0.1 MPa=10^5 Pa

1 Gal=1 cm/s^2=10^{-2} m/s^2

1 Ci=3.7×10^{10} Bq

1 R=2.58×10^{-4} C/kg

1 rad=1 cGy=10^{-2} Gy

1 rem=1 cSv=10^{-2} Sv

表5　SI接頭語

倍数	接頭語	記号
10^{18}	エクサ	E
10^{15}	ペタ	P
10^{12}	テラ	T
10^{9}	ギガ	G
10^{6}	メガ	M
10^{3}	キロ	k
10^{2}	ヘクト	h
10^{1}	デカ	da
10^{-1}	デシ	d
10^{-2}	センチ	c
10^{-3}	ミリ	m
10^{-6}	マイクロ	μ
10^{-9}	ナノ	n
10^{-12}	ピコ	p
10^{-15}	フェムト	f
10^{-18}	アト	a

（注）

1. 表1－5は「国際単位系」第5版，国際度量衡局 1985年刊行による。ただし，1 eVおよび1 uの値はCODATAの1986年推奨値によった。
2. 表4には海里，ノット，アール，ヘクタールも含まれているが日常の単位なのでここでは省略した。
3. barは，JISでは流体の圧力を表わす場合に限り表2のカテゴリーに分類されている。
4. EC閣僚理事会指令ではbar，barnおよび「血圧の単位」mmHgを表2のカテゴリーに入れている。

換算表

力	N(=10^5 dyn)	kgf	lbf
	1	0.101972	0.224809
	9.80665	1	2.20462
	4.44822	0.453592	1

粘度　1 Pa·s(N·s/m^2)=10 P(ポアズ)(g/(cm·s))

動粘度　1 m^2/s=10^4 St(ストークス)(cm^2/s)

圧力	MPa(=10 bar)	kgf/cm^2	atm	mmHg(Torr)	lbf/in^2(psi)
	1	10.1972	9.86923	7.50062×10^3	145.038
	0.0980665	1	0.967841	735.559	14.2233
	0.101325	1.03323	1	760	14.6959
	1.33322×10^{-4}	1.35951×10^{-3}	1.31579×10^{-3}	1	1.93368×10^{-2}
	6.89476×10^{-3}	7.03070×10^{-2}	6.80460×10^{-2}	51.7149	1

エネルギー・仕事・熱量	J(=10^7 erg)	kgf·m	kW·h	cal(計量法)	Btu	ft·lbf	eV
	1	0.101972	2.77778×10^{-7}	0.238889	9.47813×10^{-4}	0.737562	6.24150×10^{18}
	9.80665	1	2.72407×10^{-6}	2.34270	9.29487×10^{-3}	7.23301	6.12082×10^{19}
	3.6×10^6	3.67098×10^5	1	8.59999×10^5	3412.13	2.65522×10^6	2.24694×10^{25}
	4.18605	0.426858	1.16279×10^{-6}	1	3.96759×10^{-3}	3.08747	2.61272×10^{19}
	1055.06	107.586	2.93072×10^{-4}	252.042	1	778.172	6.58515×10^{21}
	1.35582	0.138255	3.76616×10^{-7}	0.323890	1.28506×10^{-3}	1	8.46233×10^{18}
	1.60218×10^{-19}	1.63377×10^{-20}	4.45050×10^{-26}	3.82743×10^{-20}	1.51857×10^{-22}	1.18171×10^{-19}	1

1 cal = 4.18605 J（計量法）

= 4.184 J （熱化学）

= 4.1855 J （15 °C）

= 4.1868 J（国際蒸気表）

仕事率　1 PS（仏馬力）

= 75 kgf·m/s

= 735.499 W

放射能	Bq	Ci
	1	2.70270×10^{-11}
	3.7×10^{10}	1

吸収線量	Gy	rad
	1	100
	0.01	1

照射線量	C/kg	R
	1	3876
	2.58×10^{-4}	1

線量当量	Sv	rem
	1	100
	0.01	1

（86年12月26日現在）

High Efficiency, High Energy Second-harmonic Generation of Nd : glass Laser Radiation in Large Aperture $CsLiB_6O_{10}$ Crystals